Observation of Global Alfvén Eigenmode Avalanche events on the National Spherical Torus Experiment

E. D. Fredrickson 1), N. Gorelenkov 1), E. Belova 1), N. A. Crocker 2), S. Kubota 2), B. LeBlanc 1), R. E. Bell 1), D. R. Smith 1), M. Podesta 1), H. Yuh 3), F. Levinton 3)

1) Princeton Plasma Physics Laboratory, Princeton New Jersey 08543
2) Univ. of California, Los Angeles, CA 90095
3) Nova Photonics, Princeton, NJ 08543

email contact of main author: efredrickson@pppl.gov

Abstract. Instabilities excited by the fast-ion population on NSTX [M. Ono, et al., Nucl. Fusion **40** 557 (2000)] extend from low frequency Energetic Particle Modes (EPMs) at 10's of kHz, through Toroidal Alfvén Eigenmodes [TAE] in the range of 50kHz to 150kHz to Global and Compressional Alfvén Eigenmodes [GAE and CAE] in the frequency range of 0.3MHz to 2.5MHz, or roughly $0.1\omega_{ci}$ to $0.7\omega_{ci}$. The GAE instabilities exhibit complex non-linear behavior, including onset of strong growth above an amplitude threshold. This is conjectured to occur when resonance regions in phase space start to overlap, resulting in enhanced rapid growth and redistribution of energetic particles, a process referred to as an 'avalanche' [Berk, *et al*., Nucl. Fusion **35** (1995) 1661]. The GAE are suppressed following the avalanche, suggesting depletion of the fast ion population resonantly driving the modes, and in some instances the GAE bursts appear to trigger lower frequency TAE avalanches or Energetic Particle Modes, suggesting some significant redistribution of fast ions in phase space has occurred. This paper also provides the first measurements of internal GAE mode structure showing that the mode amplitude peaks towards the plasma core.

1. INTRODUCTION

The National Spherical Torus Experiment (NSTX) [1] is a low aspect ratio ($A = R/a \approx 1.5$) tokamak with maximum toroidal field of up to 5.5kG, plasma current of up to ≈1.2MA and neutral beam injection (NBI) heating of up to ≈ 6MW with 60kV to 90kV deuterium neutral beams. The relatively low field and high beam voltage result in a population of super-Alfvénic fast ions (ions with velocity greater than the Alfvén speed), much as is expected for many fusion reactor concepts. A wide range of instabilities excited by the fast ion population has been seen on NSTX [2], and other low aspect ratio tokamaks like MAST [3] and START [4].

Instabilities excited by the fast-ion population in NSTX discussed here include Toroidal Alfvén Eigenmodes [TAE] and Global or Compressional Alfvén Eigenmodes [GAE and CAE] in the frequency range of 0.83 MHz to 1.2 MHz, or roughly $0.25\omega_{ci}$ to $0.35\omega_{ci}$. Fast ion driven instabilities on NSTX typically exhibit bursting, frequency chirping (up and/or down) and in some cases, avalanching (a slow build-up in amplitude

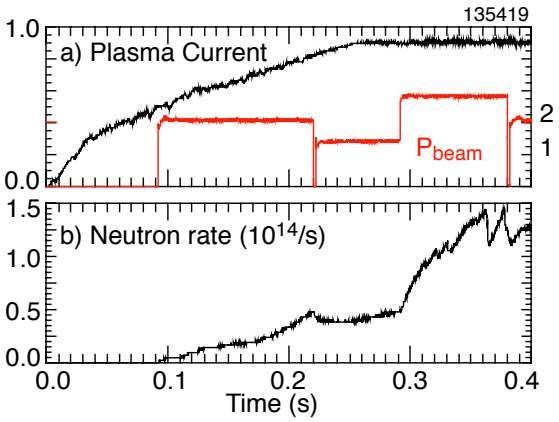

Fig. 1. a) Plasma current and heating beam power profile, b) neutron rate.

culminating in a final, rapid growth of one or more modes followed by a quiescent period [5]).

Global and Compressional Alfvén Eigenmodes are of interest for their possible roles in anomalous losses of fast ions, enhancement of electron thermal diffusivity, "alpha-channeling", or stochastic heating of thermal ions. Fast ion driven modes remove energy from the fast ions, changing their orbits which can affect confinement. The trapped electron bounce frequency can be comparable to the GAE and CAE mode frequencies, resulting in the potential for resonantly enhanced trapped electron transport [6]. Fast ions heat thermal electrons through collisional slowing down, however, waves offer the opportunity to direct the power flow from the fast ion distribution directly to the thermal ions, avoiding the lossy electron channel, through various proposed "alpha-channeling" processes [7].

The plasma current, beam heating profile in time and neutron rate from a representative shot with GAE avalanches is shown in Fig. 1. The time history of beam voltage and power was optimized to excite TAE avalanches, and both TAE and GAE avalanching behavior is present. The small drops in neutron rates from 0.3 to 0.35s coincide with TAE avalanches.

2. Experimental Observations

The diagnostics on NSTX with the bandwidth and sensitivity to study modes in the MHz frequency range include the Mirnov coil arrays (for detection and measurement of poloidal and toroidal wavelengths and the polarization of the magnetic fluctuations) and the reflectometer arrays and the Beam Emission Spectroscopy (BES) diagnostic (for measurement of the internal mode amplitude and radial structure). The reflectometers provide the most sensitive measurement of internal mode structure and amplitude, but their use constrains the plasmas being studied to peaked density profiles (L-mode).

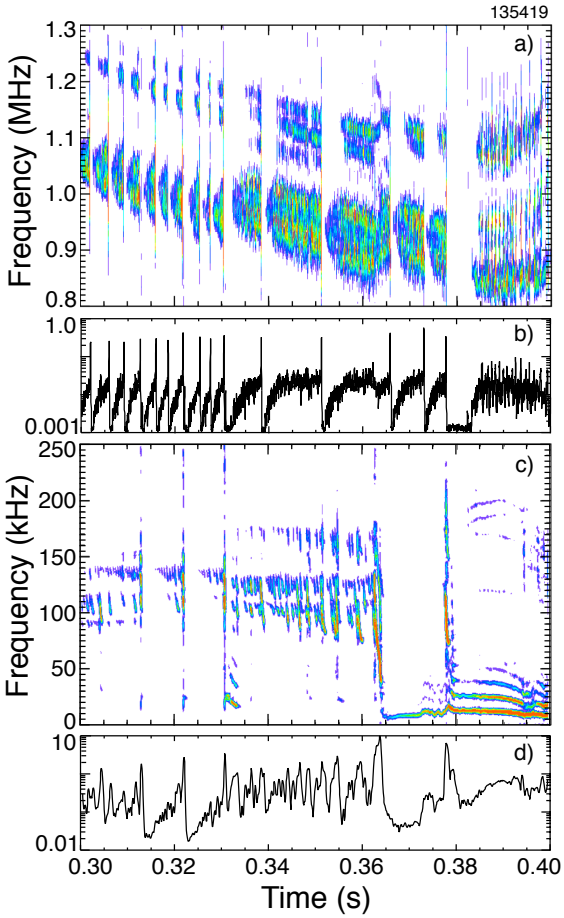

Fig. 2. a) spectrogram showing GAE modes, b) rms magnetic fluctuations 0.8MHz<freq<1.3MHz, c) spectrogram showing TAE and low frequency kink activity, d) rms magnetic fluctuations from 30kHz<freq< 200 kHz.

However, internal fluctuations of GAE modes during the large amplitude phase of an avalanche have also been measured in H-modes with the BES diagnostic.

GAE and TAE avalanches detected with a Mirnov coil are shown in Fig. 2. The spectrogram in Fig. 2a and rms fluctuation level in Fig. 2b show GAE avalanches in an L-mode plasma. Similarly, Fig. 2c shows a spectrogram with five TAE avalanches over the same time interval, and Fig. 2d shows the rms fluctuations in the TAE frequency band.

The GAE avalanche period starts off short, about 3 ms, and then lengthens to about 15 ms. However, the amplitude of the magnetic fluctuations in the final avalanche bursts, which appear as spikes in the rms plot (Fig. 2b), remain relatively constant.

The GAE amplitude increases nearly exponentially between avalanches (that is nearly linearly in the semi-logarithmic plot, Fig. 2b), reaching nearly the same amplitude before the growth of the final burst is triggered. In later avalanche periods, the mode amplitude can also saturate for some time before the avalanche burst is triggered.

Neutron rate drops, or evidence of fast ion redistribution or loss in the FIDA diagnostic or sFLIP data, are not seen with the GAE avalanches. However, the GAE-quiescent period following each strong burst is consistent with a fast-ion redistribution which reduces the free-energy available to drive the modes.

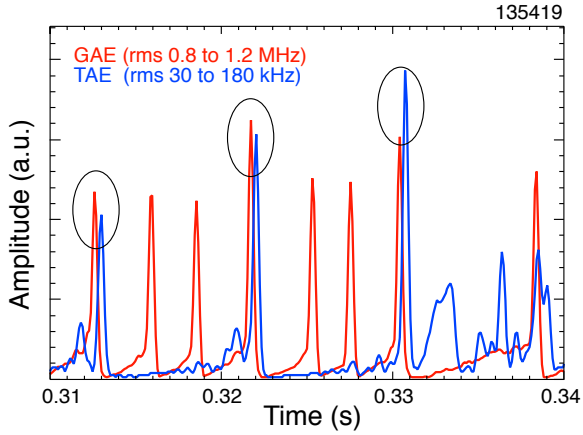

Fig. 3. RMS fluctuation levels in GAE frequency band (red) and TAE frequency band (blue). Relative fluctuation amplitudes between red/blue curves is arbitrary; shown for timing only.

Additional indirect evidence of fast ion redistribution is shown in Fig. 3, where the rms fluctuation level for GAE (red) and TAE (blue) are shown. The three TAE avalanche events in this time range are seen as spikes in the blue curve, highlighted at their tips by the black ovals. Each of the three TAE avalanches follows a GAE avalanche by approximately one hundred microseconds, although not every GAE avalanche has a corresponding TAE avalanche. The timing suggests that the redistribution of fast ions from the GAE avalanche provided some of the impetus to trigger the TAE avalanche. There are three TAE avalanches in this time period, at

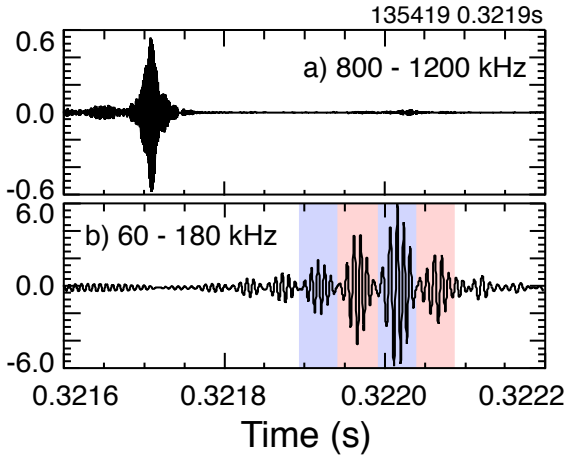

Fig. 4. Mirnov coil digitally bandpass filtered in three ranges showing a) GAE burst, b) TAE avalanche.

0.313s, 0.322s, and 0.331s, each with its concomitant drop in the neutron rate, indicative of fast ion losses.

The Mirnov signal through GAE and TAE avalanche events is shown in more detail in Fig. 4. The Mirnov coil signal is digitally filtered into two frequency bands. The GAE avalanche burst is seen in the frequency band from 0.8 MHz to 1.2 MHz (Fig. 4a) and the TAE avalanche burst in the range from 60 kHz to 180 kHz (Fig. 4b). It's clear that the GAE burst precedes the onset of the TAE avalanche. The amplitude modulation of the TAE fluctuations is due to the beating of the dominant, nearly equal amplitude n=3 and n=4 modes.

In Figs. 5a and 5b is shown a trace of the phase fluctuations from a quadrature reflectometer signal showing the final, large burst of a GAE avalanche at 0.366s. The burst is shown on a short time scale in Fig. 5a, where growth and decay times of ≈11 μs are seen. The spectrogram in Fig. 5c shows a full GAE avalanche cycle from 0.366s to 0.373s. The pre-avalanche fluctuations are seen to occupy a frequency band from ≈ 0.85 MHz to ≈ 1 MHz, in which are multiple bursting and chirping modes. These fluctuations are a mix of toroidal mode numbers, dominantly n=9 and n=11. The rms fluctuation amplitude is shown in Fig. 5d on a semi-logarithmic scale. The GAE amplitude nearly saturates before the

jump in mode amplitude by roughly an order of magnitude at the end of the avalanche cycle.

The toroidal mode number and

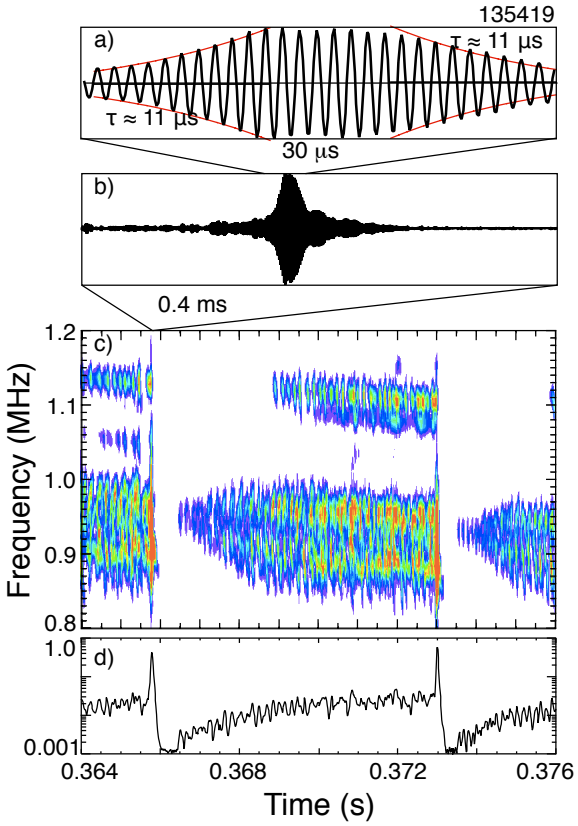

Fig. 5. a) final GAE avalanche burst measured with reflectometer with growth and decay rates of ≈ 0.9×10^5/s indicated, b) longer time period showing extended decay period, c) spectrogram over GAE avalanche cycle, rms amplitude evolution on semi-logarithmic scale.

polarization of the magnetic fluctuations are measured with a toroidal array of eight Mirnov coils, six oriented to measure the poloidal component (black points in Fig. 6) and two oriented to measure the toroidal component of the magnetic fluctuations (red points in Fig. 6). The mode is mostly compressional at the plasma edge; the dominant magnetic perturbation in the final burst in a later avalanche (0.366s) is larger parallel to the equilibrium magnetic field than in the transverse direction. The best fit to the toroidal mode number of the magnetic fluctuations is n = +7, where the positive sign denotes propagation counter to the plasma current and co-tangential beam

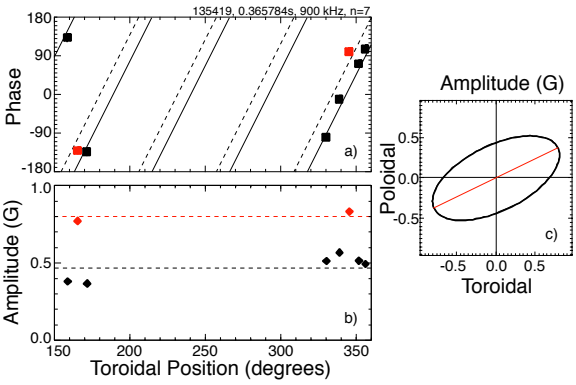

Fig. 6. a) Relative phase data from Mirnov coil array. Red points are toroidally-oriented coils, black poloidal, b) fluctuation amplitude in Gauss, c) composite Lissajous figure based on amplitude and phase data.

ions. However, decomposing the signal into the n='odd' and n='even' components, shown in Fig. 7, demonstrates that there is a significant even component to the mode, and likely an additional n=7±2 component

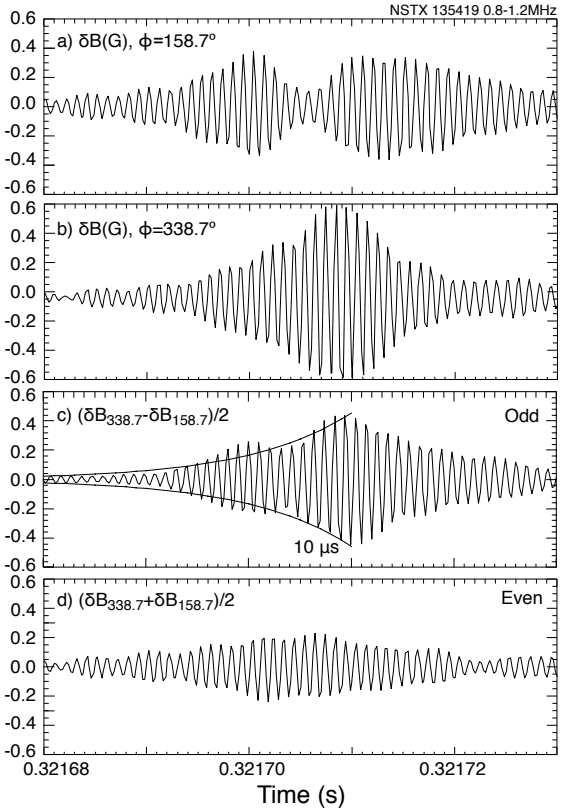

Fig. 7. a) digitally filtered Mirnov coil signal from toroidal angle of 171.5°, b) similar from 351.5°, c) Even component of final GAE avalanche burst with growth rates of 10^5/s and 2×10^5/s indicated, d) odd component (from Mirnov coils).

is inferred from the amplitude modulation of the n='odd' component.

The amplitude evolution and radial profile are measured with the five-channel reflectometer system. The displacement profile obtained with the reflectometer array is shown in Fig. 8a. The red squares are the phase fluctuation amplitudes from the quadrature reflectometer channels, converted by the free-space wavelength to an effective displacement in mm. The solid blue curve is the displacement corrected for interferometric contributions by inverting the reflectometer response to obtain the density perturbation. The simulated reflectometer response inferred from the inverted reflectometer data is shown by the red curve and is a good fit to the experimental points. Here, the displacement is the displacement of the "constant density" contours, which only corresponds to actual flux surface displacement if the waves have no compressional terms.

The relative phases of the five channels are shown in Fig. 8b and within the measurement uncertainty there is no radial propagation or nodes in the mode structure. The density profile and perturbation used to simulate the reflectometer response is shown in Fig. 8c. The inferred density perturbation is multiplied by 50 (solid black curve) to be visible in this figure, and the perturbed density is $\delta n/n \approx 1\%$. The q-profiles deduced from equilibrium reconstructions constrained with MSE data, starting 20 ms later when MSE data becomes available, are shown in Fig. 8d.

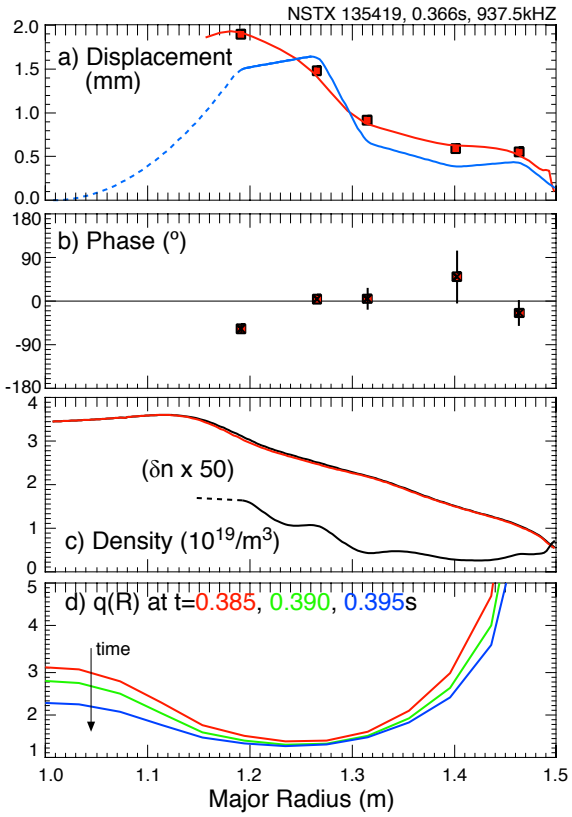

Fig. 8. a) Mode amplitude profile from reflectometer array, b) relative phase of mode, c) density profile, d) q-profile from equilibrium reconstruction with MSE pitch-angle data.

3. Discussion and analysis

These observations of GAE activity are relevant to the physics of fast-ion avalanches, stochastic ion heating, alpha-channeling, and fast ion redistribution. The measurements of mode structure and mode amplitude evolutions are important to these various areas of fast particle driven mode physics, but a detailed examination of their important is outside the scope of this paper. The identification of the modes, the resonant drive for the modes and a simple estimate for power flow through the modes are discussed.

The profile of the internal density fluctuation is measured with the reflectometer array, and the magnetic fluctuations are measured externally with Mirnov coils. There are no reflectometer measurements for $R < 1.2$m, but this data indicates that the density fluctuations peak near or inside the region of q_{min}. This would be consistent with identification of these modes as GAE, rather than CAE, which should have had a peak in amplitude further out. The pitch of the magnetic field perturbation measured at the plasma wall indicates that the mode has some compressional component, whereas GAE are in principal shear Alfvén waves.

However, toroidicity, magnetic shear and finite beta are observed to introduce compressional components in numerical simulations of GAE for NSTX parameters [8].

The pitch of fast ions resonant with the mode can be estimated from the local GAE dispersion relation $\omega = k_{||} V_{Alfvén}$ and the Doppler-shifted cyclotron resonance condition, $\omega = \omega_{ci} - k_{||}V_{b||}$. The resonant pitch is then $V_{b||}/V_b = (\omega_{ci} - \omega)/\omega$ $(V_{Alfvén}/V_b)$. For the dominant n = 9 mode in the avalanche burst, this gives a pitch of $V_{b||}/V_b \approx 0.72$ for the resonant 80 keV fast ions. As the ion energy drops, the pitch required for resonance increases. The fast ion

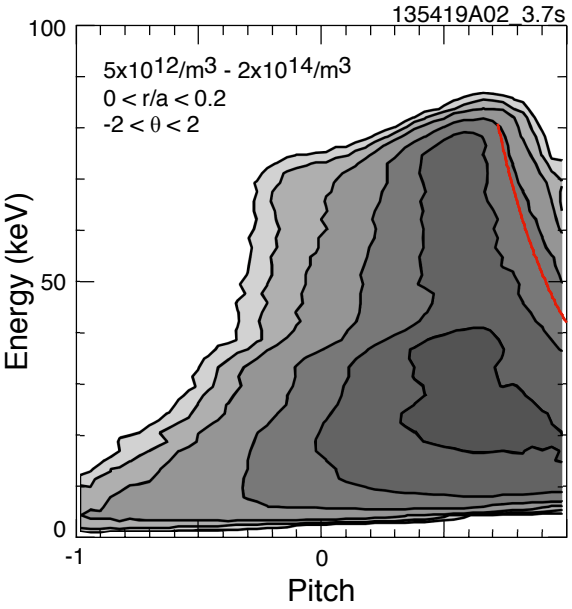

Fig. 9. Distribution function calculated with the TRANSP beam deposition code. Red curve indicates fast ions resonant with dominant n = 9 mode.

distribution function calculated in TRANSP is shown in Fig. 9 and the resonant condition as a function of energy is indicated by the red line. As the resonant drive takes predominantly perpendicular energy from the fast ions, the result is to reduce the poloidal gyro-radius and improve the fast ion confinement. Note that to satisfy this resonance condition, the wave must propagate counter to the beam ion direction, as is experimentally measured.

The early GAE amplitude evolution is suggestive of avalanching behavior, with a slow growth in mode amplitude as the fast ion population builds up, leading to a short, explosive growth to much larger amplitude which is then followed by a quiescent period. After 0.33s, however, the slow growth seems to saturate for an extensive period of time. This could be explained if the mode amplitude saturated just below the threshold for triggering an avalanche, that is before resonance islands in fast ion phase space begin to overlap. An intriguing alternative explanation is that this represents the "stochastic thermal ion heating" threshold [9]. At this amplitude, there is an effective damping term increasing strongly with mode amplitude as the wave dumps energy into the thermal ion population. In the 'linear' regime, the mode drive is fixed or falling with mode amplitude, this quickly leads to saturation. However, extensive simulations are needed to examine this hypothesis. The potential effective heating power is estimated below, but depending upon how far below the 'natural' saturation amplitude the stochastic threshold is, a still substantial portion of the power will go to the electrons through Landau damping.

The avalanches in the time period from 0.33s to 0.37s appear coincidently, or follow, bursts of lower frequency (TAE) activity. The presence of multiple modes in the final, large bursts, is indicated by the amplitude modulations of the even and odd signals. The presence of the multiple modes complicates the measurement of the growth and damping rates in the final burst. However, the observed growth and decay of the final bursts appears roughly symmetrical, with growth and decay times of approximately 10 μs, or $\gamma/\omega \approx 3.4\%$. If the assumption is made that the drive is negligible during the burst decay, Fig. 4a suggests that the peak drive, γ_{drive} is

approximately twice the damping rate, γ_{damp}, *e.g.*, $\gamma_{growth} = \gamma_{drive} - \gamma_{damp} \approx \gamma_{damp} \approx 10^5/s$. This is a minimum estimate for damping and drive; the actual damping and drive terms could be larger.

The peak mode amplitude of $\delta n/n \approx 1\%$ can be used to estimate the magnetic fluctuation level, which together with the growth/damping rate estimate can be used to calculate the approximate power flow from the fast ion population through the mode and into the thermal plasma. For compressional modes, the relation is $\delta B/B \approx \delta n/n$, for shear modes, the relation is more complicated, but roughly $\delta B/B \approx L_n/L_B\ \delta n/n$, where L_B is the relevant magnetic gradient scale length. As the magnetic gradient scale length is typically greater than the density gradient scale length, the magnetic perturbations for shear waves would generally be weaker, for a given density perturbation, than for compressional waves. In the following discussion, we use the larger estimate for magnetic fluctuations from the compressional approximation to give an upper estimate for energy in the mode. The peak amplitude of $\delta n/n \approx 1\%$ implies $\delta B \approx 40G$.

The total energy density in the wave may be estimated as twice $4x10^{-3}$ J/m^3G^2 $(40\ G)^2 \approx 13\ J/m^3$. The wave amplitude is small outside of $R \approx 1.3m$, thus the plasma volume where mode amplitude is significant is $\approx 2\pi R\ \pi r^2\ \kappa \approx 3.2\ m^3$ ($R=1m$, $r=0.3m$, $\kappa = 1.8$), giving a the wave stored energy of $\approx$ 40 J. These estimates are very approximate, but suggest that $\approx$ 40 J of energy is transferred from the fast ion population to the wave, and then to the thermal plasma at each GAE avalanche event. The ten avalanche events between 0.3 and 0.33s give an effective heating power of 0.4 kJ/ 0.03s $\approx$ 13 kW. The peak heating power from the pre-avalanche phase, assuming an effective damping rate of 10^5/s, and roughly 10% of the amplitude reached during the avalanche, is $\approx$ 50kW, although the time average would be less. Much of this power is assumed to go to the electrons through electron Landau damping, but these power flow estimates are much less than the total neutral beam heating power at this time of 2MW.

4. Summary

A broad spectrum of modes in the frequency range from 0.5 MHz to 1.5 MHz is often seen in NSTX beam heat plasmas. The modes are surmised to be Global Alfvén Eigenmodes based on their spectrum and evolution of frequencies. The modes exhibit a range of behavior, including chirping and bursting as well as more continuous activity. In this paper we have presented data documenting behavior characterized as avalanching, a slow growth in mode amplitude following a quiescent period, culminating in very rapid growth of multiple modes leading again to a quiescent period. The avalanches are seen to involve multiple modes with toroidal mode numbers from roughly n=7 to n=11.

The modes are postulated to be excited through a Doppler-shifted cyclotron resonance with beam ions. We have estimated the pitch-angle of fast ions satisfying this resonance condition and shown that it aligns well with the distribution of fast ions calculated with the TRANSP code. We deduce that these avalanches redistribute fast ions from the quiescent period following the avalanche burst and by the apparent triggering of TAE mode avalanches at lower frequency. So far there are no direct measurements of fast ion redistribution with neutron rate, a scintillator-based lost ion probe or NPA diagnostics. However, it is quite possible that the fast ion redistribution results in improved confinement, as the cyclotron resonance should increase the pitch of fast ions, making their velocities more parallel and generally better confined.

The GAE are expected to be localized near the low shear region of minimum q.

Internal measurements show that the modes are indeed peaked toward magnetic axis, possibly near the off-axis minimum in q. The peak mode amplitude as measured with the reflectometers reaches $\delta n/n \approx 1\%$.

The authors are grateful to the NSTX team for supporting these experiments. Work supported by U.S. DOE Contracts DE-AC02-76CH03073, DE-FG03-99ER54527, DE-FG02-06ER54867, and DE-FG02-99ER54527.

5. Acknowledgements

6. Bibliography

[1] M. Ono, S.M. Kaye, Y.-K.M. Peng, G. Barnes, W. Blanchard, M.D. Carter, J. Chrzanowski, L. Dudek, R. Ewig, D. Gates, R.E. Hatcher, T. Jarboe, S.C. Jardin, D. Johnson, R. Kaita, M. Kalish, C.E. Kessel, H.W. Kugel, R. Maingi, R. Majeski, J. Manickam, B. McCormack, J. Menard, D. Mueller, B.A. Nelson, B.E. Nelson, C. Neumeyer, G. Oliaro, F. Paoletti, R. Parsells, E. Perry, N. Pomphrey, S. Ramakrishnan, R. Raman, G. Rewoldt, J. Robinson, A.L. Roquemore, P. Ryan, S. Sabbagh, D. Swain, E.J. Synakowski, M. Viola, M. Williams, J.R. Wilson and the NSTX Team, Nucl. Fusion 40 (2000) 557.

[2] E. D. Fredrickson, N. A. Crocker, R. E. Bell, D. S. Darrow, N. N. Gorelenkov, G. J. Kramer, S. Kubota, F. M. Levinton, D. Liu, S. S. Medley, M. Podestá, K. Tritz, R. B. White, and H. Yuh Phys. of Plasmas **16** (2009), 122505.

[3] Sharapov, S.E., Alper, B., Andersson, F., Baranov, Yu.F., Berk, H.L., Bertalot, L., Borba, D., Boswell, C., Breizman, B.N., Buttery, R., Challis, C.D., de Baar, M., de Vries, P., Eriksson, L.-G., Fasoli, A., Galvao, R., Goloborod'ko, V., Gryaznevich, M.P., Hastie, R.J., Hawkes, N.C., Helander, P., Kiptily, V.G., Kramer, G.J., Lomas, P.J., Mailloux, J., Mantsinen, M.J., Martin, R., Nabais, F., Nave, M.F., Nazikian, R., Noterdaeme, J.-M., Pekker, M.S., Pinches, S.D., Pinfold, T., Popovichev, S.V., Sandquist, P., Stork, D., Testa, D., Tuccillo, A., Voitsekhovich, I., Yavorskij, V., Young, N.P., Zonca, F., Nuclear Fusion Sept. 2005, Vol. 45, no.9, pp. 1168-77.

[4] M P Gryaznevich and S E Sharapov, Nuclear Fusion **40** (2000) 907.

[5] H. L. Berk, B. N. Breizman, M. Pekker, Phys. Plasmas **2**, 3007 (1995)

[6] D. Stutman, L. Delgado-Aparicio, N. Gorelenkov, M. Finkenthal, E. Fredrickson, S. Kaye, E. Mazzucato, and K. Tritz, Phys. Rev. Lett. 102, 115002 (2009).

[7] N N Gorelenkov, N J Fisch and E Fredrickson, Plasma Phys. Control. Fusion 52 (2010) 055014.

[8] E Belova, N N Gorelenkov, C Z Cheng, E D Fredrickson, in Proceedings of the 30th European Physical Society Conference on Controlled Fusion and Plasma Physics, St. Petersburg, Russia, July 2003, ECA Vol. 27A, P-3.102.

[9] G R Smith, A N Kaufman, Phys. Rev. Lett. 34 (1975) 1613.